Role of Conserved E2 Residue W420 in Receptor Binding and Hepatitis C Virus Infection

Vanessa M. Cowton[1], Allan G.N. Angus[1], Sarah J. Cole[1], Christina K. Markopoulou[1], Ania Owsianka[1], James I. Dunlop[1], Deborah E. Gardner[1], Thomas Krey[2,3,4,5] and Arvind H. Patel[1]#

[1]MRC - University of Glasgow Centre for Virus Research, Garscube campus, 464 Bearsden Road, Glasgow, G61 1QH, UK

[2]Institut Pasteur, Unité de Virologie Structurale, Department Virologie, Paris, France

[3]CNRS UMR 3569, Paris, France

[4]Institute of Virology, Hannover Medical School, Hannover, Germany

[5]German Centre for Infection Research (DZIF), partner site Hannover-Braunschweig

Running Head: Mutagenesis of Conserved Residue W420 in HCV E2

#Address correspondence to Arvind H. Patel, e-mail: arvind.patel@glasgow.ac.uk,

Abstract count - 250 words;

Importance count -131 words

Text count - 6819 words

ABSTRACT

Hepatitis C virus (HCV) enters cells via interactions with several host factors, a key one being that between the viral E2 envelope glycoprotein and the CD81 receptor. We previously identified the E2 tryptophan 420 (W420) as an essential CD81-binding residue. However, the importance of W420 in the context of the native virion is unknown as these earlier studies predate the infectious HCV cell-culture (HCVcc) system. Here, we introduced four separate mutations (F, Y, A or R) at position 420 within the infectious JFH-1 HCVcc genome and characterized their effects on the viral cycle. Whilst all mutations reduced E2-CD81 binding, only two (W420A and W420R) reduced HCVcc infectivity. Further analyses of mutants with hydrophobic residues (F or Y) found that interactions with receptors SR-BI as well as CD81 were modulated which in-turn determined the viral uptake route. Both mutant viruses were significantly less dependent on SR-BI, and its lipid-transfer activity, for virus entry. Furthermore, they were resistant to the drug erlotinib that targets EGFR (a host co-factor for HCV entry) and also blocks SR-BI dependent HDL-mediated enhancement of virus entry. Together, our data indicate a model where alteration at position 420 causes a subtle change in E2 conformation that prevents interaction with SR-BI and increases accessibility to the CD81 binding site in-turn favoring a particular internalization route. They further show that a hydrophobic residue with a strong preference for tryptophan at position 420 is important, both functionally and structurally, to provide an additional hydrophobic anchor to stabilize the E2-CD81 interaction.

IMPORTANCE

Hepatitis C virus (HCV) is a leading cause of liver disease causing up to 500000 deaths annually. The first step in the viral life-cycle is the entry process. This study

investigates the role of a highly conserved residue, tryptophan 420 of the viral glycoprotein E2 in this process. We analyzed the effect of changing this residue in the virus and confirmed that this region is important for binding to the CD81 receptor. Furthermore, alteration of this residue modulated the interaction with the SR-BI receptor and changes to these key interactions were found to affect the virus internalization route involving the host co-factor, EGFR. Our results also show that the nature of the amino acid at this position is important functionally and structurally to provide an anchor-point to stabilize the E2-CD81 interaction.

INTRODUCTION

HCV is a positive-strand RNA virus belonging to the *Hepacivirus* genus within the *Flaviviridae* family (1).The viral genome comprises a single open reading frame (ORF), encoding structural and non-structural (NS) proteins, flanked by two untranslated regions (UTRs) at the 5' and 3' ends. The large polyprotein of approximately 3000 amino acids [aa] is cleaved by cellular and viral proteases into 10 different proteins: core, E1, E2, p7, NS2, NS3, NS4A, NS4B, NS5A, and NS5B (2).The structural proteins include core, which forms the viral nucleocapsid and the envelope glycoproteins E1 and E2 that mediate early cell entry events (3). NS2 and p7 (a viroporin) play crucial roles in virus assembly/egress (4-6) and the remaining non-structural proteins NS3, NS4A, NS4B, NS5A, and NS5B form replication complexes, which synthesize both plus and minus-strand viral RNAs (7). HCV is classified into seven major genetic groups and further subdivided into numerous subtypes (1, 8). This genetic variability is caused by the error-prone nature of the RNA-dependent RNA polymerase (NS5B), amplified by the high viral production rate (9) and further accelerated by the selective pressure exerted by the host immune response (10).

The viral particle consists of a nucleocapsid encasing the viral RNA, surrounded by a lipidic cell-derived envelope in which the glycoproteins E1 and E2 are embedded. Numerous reports have shown that both serum- and cell-culture-derived HCV (HCVcc) are tightly associated with low density lipoproteins (LDLs) and very low density lipoproteins (VLDLs) to form a hybrid particle called a lipoviroparticle (LVP) (11, 12). *In vivo*, these associations are believed to protect HCV from the humoral immune response by shielding the glycoproteins from circulating neutralizing antibodies (nAbs) (3). HCVcc studies have also shown that the major VLDL component, apoE, functions in the viral entry process (13). HCV entry into hepatocytes is a multi-step process involving a series of interactions between the virus particles and several cellular molecules. Initial attachment of HCV to the cell surface most likely occurs via interactions between virion-associated apoE with low-density-lipoprotein receptor (LDLR) and with glycosaminoglycans (GAGs), present on heparan sulfate proteoglycans (HSPGs) (14-18). To gain entry into the cell, HCV depends on several cellular molecules: scavenger receptor BI (SR-BI) (19); tetraspanin CD81 (20); tight junction proteins claudin-1 (21) and occludin (22); epidermal growth factor receptor (EGFR) (23) and its signal transducer Harvey rat sarcoma viral oncogene homolog (HRas) (24); Niemann–Pick C1-like cholesterol receptor (NPC1L1) (25) and transferrin receptor 1 (26). The interaction of HCV particles with the cell leads to the internalization of particles through clathrin-mediated endocytosis (27, 28) and their subsequent fusion at low pH with the membranes of early endosomes (29). Only two of these host cell molecules, CD81 and SR-BI have been reported to interact directly with the HCV envelope glycoproteins (19, 20). SR-BI mediates binding of E2 through an interaction that

involves the hypervariable region 1 (HVR1), a 27 amino acid segment located at the N-terminus of the HCV E2 glycoprotein. It is believed that HVR1 masks or induces masking of the E2-CD81 binding site and that the E2-SR-B1 interaction facilitates conformational changes within the glycoproteins that cause exposure of the CD81 binding site (30). CD81 has been demonstrated to have a major role in HCV entry and is the best characterized of the cellular entry factors to date. Numerous studies have identified E2 regions and residues that are potentially involved in CD81 interaction based on the characterization of neutralizing antibodies, mutagenesis studies, and structural data (31). However, most of these studies used soluble E2 or HCV pseudoparticle (HCVpp)-derived E2 in which the conformation of E2 is slightly different from the envelope glycoproteins in native HCV particles (32). Therefore, it remains unclear which E2 residues or sequences are genuinely involved in the interaction of virus particles with CD81. Prior to the availability of the HCVcc system we identified several residues required for E2-CD81 binding by alanine mutagenesis (33). One of these residues, W420, was located within the highly conserved E2 epitope I, comprising residues 412-423. We also showed that the mouse monoclonal antibody (mAb) AP33, which inhibits the E2-CD81 interaction, bound to this epitope and specifically recognized residues L413, N415, G418 and W420 (33, 34). Analysis of amino acid variation within the AP33 epitope shows that W420 is 99.9% conserved (35), which suggests that it is functionally or structurally important. Epitope mapping has shown it to be a contact residue for several broadly neutralizing antibodies, including AP33 (reviewed in (36)). More recently this has been confirmed by structural analysis, which reveals how extensively this residue is bound by the neutralizing antibodies that recognize this epitope (35, 37-40).

To further investigate the role of W420 in CD81 binding and virus infection, we substituted this residue with phenylalanine, tyrosine, alanine or arginine in the genotype 2a HCVcc JFH-1 background. We then characterized the mutant viruses by testing their viral replication levels, cellular receptor interactions and sensitivity to neutralizing antibodies. We confirmed that W420 is important for CD81 binding during virus entry and interestingly also modulates virion interaction with receptor molecules SR-BI and EGFR. Together, our results suggest that the tryptophan as a large hydrophobic residue functions in conjunction with other CD81-binding regions to provide an additional anchor-point to stabilize the E2-CD81 interaction.

MATERIAL AND METHODS

Cells. Human epithelial kidney cells (HEK)-293T (ATCC CRL-1573), human hepatoma Huh-7 (41) and Huh7-J20 (42) were propagated in Dulbecco's modified essential medium supplemented with penicillin/streptomycin, non-essential amino acids and 10% fetal calf serum (DMEM). CHO-K1 cells were propagated in HAM F-12 medium (Life Technologies) supplemented as above. Stable cell-lines CHO-hSR-BI or CHO-hSR-BI-GFP were generated by cloning sequences encoding the human SR-BI or SR-BI-EGFP fusion protein into the retrovirus transfer vector pQCXIP (BD Biosciences). These plasmids were co-transfected with constructs expressing MLV gag-pol and vesicular stomatitis virus (VSV) G glycoprotein into HEK-293T cells to generate VSV-G pseudoparticles (VSVpp). CHO-K1 cells were transduced with VSVpp carrying the gene encoding human SR-BI or SR-BI-EGFP and transduced cells were selected in medium containing 4 μg/ml puromycin.

147 **Antibodies.** The anti-E2 rodent mAbs AP33, 3/11 and human mAb (HmAb) CBH-5
148 have been described previously (43-46). The anti-E2 mAbs CBH-5, 3/11, and the anti-
149 NS5A mAb 9E10 (47), were kindly provided by S. Foung, J. McKeating and C. M.
150 Rice, respectively. The murine leukemia virus (MLV) gag-specific mAb was obtained
151 from rat hybridoma cells (ATCC CRL-1912). The anti-core mAb C7-50, and the anti-
152 CD81 mAb JS-81 were obtained from Bioreagents and BD Biosciences, respectively.
153 The anti-Flag M2 mAb was obtained from Sigma-Aldrich. A derivative of anti-SR-BI
154 human mAb151 described previously (48) was generated in CHO-K1 cells. Briefly,
155 the variable heavy (vH) and variable light (vL) chain encoding sequences of mAb151
156 were cloned into mouse IgG1 expression vectors pFUSEss-CHIg-mg1 and
157 pFUSE2ss-CLIg-mk (InvivoGen, CA, USA), respectively. Following co-transfection
158 of these plasmids into CHO-K1 cells, a clone stably secreting the human-mouse
159 chimeric IgG (called mAb151-NP1) was selected and expanded. MAb151-NP1
160 secreted into the medium was purified using protein G-sepharose affinity
161 chromatography and confirmed to react specifically to human SR-BI. Cell-surface
162 expression of SR-BI was measured by incubating cells with anti-SR-BI mAb151-NP1
163 or an isotype IgG1 control, followed by an anti-mouse phycoerythin (PE)-conjugated
164 secondary antibody. The cells were analyzed by flow cytometry on a FACScalibur
165 with CellQuest Pro software (BD biosciences).
166
167 **Plasmid constructs and mutagenesis.** The plasmid pUC-JFH-1 carries the full-
168 length cDNA of the genotype 2a HCV strain JFH-1. The plasmid pUC-GND JFH-1 is
169 identical except for the GND mutation in the viral NS5B RNA polymerase (49). The
170 plasmids used to generate HCV pseudoparticles (HCVpp) containing the strain JFH-1
171 envelope glycoproteins have been described previously (50). Site-directed

mutagenesis was carried out by using a QuikChange-XL-II kit (Agilent Technologies) according to the manufacturer's instructions to introduce amino acid substitutions at the target sites in E2. Briefly, the amino acid substitutions W420F, W420Y, W420A, W420R and W420V in the E2-coding region were individually introduced into the plasmid pUC-JFH-1 using appropriate primers (the sequences of which are available upon request). The presence of the desired mutations in the resulting clones was confirmed by sequencing the DNA fragments spanning the mutation site and then these fragments were subcloned back into pUC-JFH-1 and the HCVpp E1E2 expression vector.

Determination of virus infectivity and RNA replication. Infectious viruses were generated by electroporation of viral RNA into Huh7 cells as previously described (49). Infectious virus titers in the cell medium were determined by infecting Huh7 cells with serially diluted inoculum followed by immunostaining for the NS5A viral protein in a focus forming unit (FFU) assay as described previously (51). The level of virus infectivity and intracellular RNA replication was determined by infecting the reporter cell line Huh7-J20 and measuring the secreted alkaline phosphatase (SEAP) activity in the culture medium at indicated times post-infection as described previously (42). To monitor virus infectivity during serial passaging, Huh7 cells electroporated with the viral RNA or inoculated with infectious virus were passaged in T80 flasks containing DMEM. At each passage the cell culture supernatants were harvested, and the released virus infectivity was determined by FFU assay. To determine the replication of each mutant virus, 2×10^6 Huh7-J20 cells were electroporated with 10 μg of viral RNA and resuspended in 4 ml of DMEM. Aliquots of 0.5 ml were then seeded into triplicate wells of a 24-well plate. Following

197 incubation at 37°C for 72 h, the virus infectivity/replication levels and infectious virus
198 yields in cell culture supernatants were determined by SEAP and FFU assay,
199 respectively. Cell-associated virus was obtained essentially as described previously
200 (52). Briefly, 3 x 10^6 Huh-7 cells were electroporated with 10 μg of viral RNA,
201 resuspended in 15 ml of DMEM, and seeded into 90-mm culture dishes. Cells were
202 harvested at 72 h postelectroporation, washed in DMEM, resuspended in 0.8 ml
203 DMEM, and freeze-thawed three times. The samples were centrifuged to remove cell
204 debris, and the supernatant was assayed by FFU assay to determine virus infectivity.
205
206 **Western blot analysis.** Western blot analysis was performed as described previously
207 (43), with some modifications. To detect intracellular antigens, cultured cells were
208 washed once in phosphate-buffered saline (PBS) and lysed directly in SDS-PAGE
209 sample loading buffer (200 mM Tris-HCl, pH 6.7; 0.5% SDS; β-mercaptoethanol;
210 10% glycerol). Lysates were homogenized by passing through a 22-gauge needle five
211 times before use. To obtain extracellular virus, 10 ml of culture medium from
212 electroporated cells was harvested, filtered, and overlaid onto 1 ml of a 20% (wt/vol)
213 sucrose cushion made with PBS and centrifuged at 25,000 rpm for 4 h in a Sorvall
214 Discovery 90SE ultracentrifuge. The pellets were then lysed directly in 50 μl of SDS-
215 PAGE sample loading buffer and stored at -20°C until use. The proteins in 20 μl of
216 sample were resolved by 12.5% SDS-PAGE and transferred onto nitrocellulose
217 membranes (Hybond-ECL; Amersham).
218
219 **Identification of reversion mutations.** Total RNA was prepared from infected cells
220 using the RNeasy kit (Qiagen), and the HCV RNA was converted to first-strand DNA
221 by using a Superscript III first-strand synthesis kit (Invitrogen) with the primer 5′-

TTGCGAGTGCCCCGGGA-3′. After digestion with 1 U of RNase H (Invitrogen) for 20 min at 37°C, one-quarter of the RT reaction was amplified with appropriate primers to yield four fragments of HCV cDNA (nucleotides [nt] 322 to 930, 538 to 3038, 2544 to 5542, and 5412 to 7890) covering the core to NS5A regions of the viral genome. The PCR products were gel purified and used directly for nucleotide sequencing.

HCVpp genesis, infection, and analysis by immunoblotting. HCVpp were generated by transfection of HEK-293T cells with plasmids expressing HCV E1E2, MLV Gag-pol and the MLV transfer vector expressing a firefly luciferase reporter. The medium containing HCVpp was collected, filtered through 0.45-μm-pore-size membrane and used to infect Huh7 cells as described previously (53). Three days after infection, the cells were lysed and their luciferase activity measured using a Bright-Glo luciferase assay system (Promega). For protein analysis, HCVpp-containing medium was pelleted through a 20% sucrose cushion (wt/vol) in PBS at 100,000 x *g* for 2 h. The pellets were resuspended in SDS-PAGE sample loading buffer and analyzed by SDS-PAGE followed by immunoblotting for HCV E2 and MLV gag.

GNA capture and CD81 binding assay. The enzyme-linked immunosorbent assay (ELISA) to detect mAb binding to E2 glycoprotein was performed essentially as described previously (54). Briefly, HEK-293T cells were cotransfected with E1E2 expression plasmids, and the expressed glycoproteins present in clarified lysates of these cells were captured onto GNA (*Galanthus nivalis* agglutinin)-coated Immulon II enzyme immunoassay (EIA) plates (Thermolabsystems). Bound glycoproteins were

247 detected using biotinylated anti-E2 mAbs, followed by Streptavidin-horseradish
248 peroxidase (Sigma-Aldrich) and TMB (3,3′,5,5′-tetramethylbenzidine; Sigma-
249 Aldrich) substrate. Absorbance values were determined at 450 nm. The E2-CD81
250 binding assay was essentially performed as above. Briefly, E1E2 from cell lysates was
251 captured onto an ELISA plate coated with GNA, the wells washed and an insect cell-
252 expressed FLAG-tagged human soluble CD81-LEL (sCD81-LEL) was added. The
253 bound CD81 was detected using anti-FLAG antibody, followed by anti-mouse-
254 horseradish peroxidase as described above.
255
256 **HCVcc neutralization assays**. Inhibition assays were performed in Huh7-J20 cells,
257 and virus infectivity levels were determined by SEAP reporter assay, as described
258 previously (42). Briefly, cells were seeded at a density of 4 x 10^3 per well in a 96-well
259 plate and incubated at 37^{o}C overnight prior to infection. For anti-E2 antibody
260 neutralization assays, virus was preincubated at 37°C for 1 h with the appropriate
261 antibody prior to infecting cells at m.o.i 0.1. To test neutralization by sCD81-LEL,
262 virus was preincubated at 37°C for 1 h with purified His-tagged sCD81-LEL
263 expressed in *E.coli* as described previously (55) prior to infecting cells at m.o.i 0.1. To
264 test neutralization by anti-receptor antibodies, cells were preincubated with
265 appropriate antibodies for 1 h at 37°C prior to infection at m.o.i 0.1. At 3 h
266 postinfection, the inoculum was replaced with fresh DMEM and incubated for 48 h.
267
268 **HCVcc dose-response assays.** BLT-4, erlotinib and sunitinib were obtained from
269 Sigma-aldrich. The assay was performed similarly to the neutralization assay
270 described above except cells were pretreated with inhibitor for 1 h at 37°C prior to
271 infection at m.o.i 0.1 for 3h, the inoculum and inhibitor was removed, cells were

washed and fresh media added. After 72 h incubation, the SEAP activity in the media was measured. Cell viability assays were performed in Huh7-J20 cells seeded at 4 x 10^3 per well in a 96-well plate and incubated at 37^{o}C overnight prior to treatment. Cells were treated with inhibitor for 4h at 37°C, washed and fresh media added. Following 72h incubation, media was removed and cells were incubated in 10% WST-1 reagent (Roche) and absorbance at 440nm measured.

RESULTS

Effects of E2 Mutations on Virus Replication. To assess the role of E2 residue W420 in virus infection, we generated HCVcc mutants containing the amino acid substitutions W420A, W420R, W420F and W420Y. Alanine, with its small, non-polar side chain is most commonly used for site-directed mutagenesis, but it is more informative to introduce residues that cover a wider range of physico-chemical properties. In this case, replacing tryptophan with the aromatic residues phenylalanine or tyrosine is a relatively conservative change. Substitution by arginine, a positively charged polar residue, is a drastic change, but we decided to include it because this mutation is found in one of 2,161 naturally occurring HCV E2 sequences (35). To study the effect of these mutations on virus replication, Huh7-J20 cells were electroporated with JFH-1_{WT}, JFH-1_{W420F}, JFH-1_{W420Y}, JFH-1_{W420A} or JFH-1_{W420R} RNA and after 72 h the supernatant was harvested for FFU and SEAP assay. All of the mutants showed SEAP activities similar to that of JFH-1_{WT} (Fig. 1a). Cells electroporated with the replication-deficient JFH-1_{GND} RNA and replication-competent but assembly-deficient JFH-$1_{\Delta E1E2}$ served as controls in this experiment. These results indicate that the E2 mutations do not alter intracellular HCV RNA replication. Similar levels of viral proteins core, E2 and NS5A were detected in all the

297 cell lysates, confirming that these mutations do not affect genome or protein synthesis
298 (Fig. 1c). In contrast, major differences were observed in the titer of infectious virus
299 released into the cell medium (Fig.1b). JFH-1_{W420F} and JFH-1_{W420Y} viruses showed
300 comparable peak titers to JFH-1_{WT}, whereas the infectivity of the JFH-1_{W420A} and
301 JFH-1_{W420R} viruses was reduced by ~1 $\log_{10}$ and ~4 $\log_{10}$, respectively. A similar
302 infectivity profile was obtained using intracellular virus (recovered from cells lysed
303 by freeze-thawing), indicating that the defect in JFH-1_{W420A} and JFH-1_{W420R}
304 infectivity is not due to reduced virion secretion (Fig. 1b). To determine whether the
305 W420 mutants were producing non-infectious viral particles, culture medium
306 harvested 72 h post-electroporation was concentrated and probed for the presence of
307 core protein by immunoblotting, and also tested for infectivity. We found that all the
308 mutants secreted levels of extracellular core protein similar to JFH-1_{WT}, whereas the
309 infectivity of JFH-1_{W420A} and JFH-1_{W420R} was very much reduced (Fig. 1c, pelleted),
310 which means that these mutations alter the specific infectivity of particles, with little
311 or no effect on virus assembly and secretion.
312
313 **Reversion of E2 mutants during prolonged culture.** To determine whether the
314 infectivity of the JFH-1_{W420A} and JFH-1_{W420R} mutants could be rescued by
315 compensatory mutations, cells electroporated with JFH-1_{W420R} RNA or infected with
316 JFH-1_{W420A} virus were serially passaged. The level of infectious virus released into
317 the culture medium was monitored throughout each passaging experiment. A
318 progressive increase in extracellular virus release was observed in both experiments
319 that eventually achieved peak titers similar to those expected for JFH-1_{WT} (data not
320 shown). To identify the mutation(s) responsible for this increased infectivity, total
321 RNAs were prepared from cells infected with virus collected from the final passage

and the core to NS5A encoding regions of the HCV genome were sequenced by RT-PCR. Interestingly, the sequencing revealed that the JFH-1_{W420R} virus had reverted back to the wild type tryptophan residue by a single nucleotide change (CGG to TGG) which emphasizes the functional importance of W420. The passaged JFH-1_{W420A} also contained a single nucleotide change (GCG to GTG) thereby converting the original alanine substitution to a valine residue. To determine if this valine substitution was indeed responsible for the improved infectivity of JFH-1_{W420A} seen during passaging, we engineered this change into the original JFH-1_{WT} genome and analyzed infectious virus production at 72 h post-electroporation. As shown in Fig. 1d the JFH-1_{W420V} mutant displayed cell-free infectivity comparable to JFH-1_{WT}, suggesting that the JFH-1_{A420V} change functions as a reversion mutation.

Infectivity Profiling in the HCVpp System

We previously showed that a W420A mutation in the HCV genotype 1a strain H77 E2 abolished HCVpp infection (33). However, the results presented here show that the same mutation in the strain JFH-1 HCVcc system only reduces infection 10-fold. To resolve this discrepancy, we assessed the infectivity of the JFH-1 E2 W420 mutants in the HCVpp system. In contrast to the results in HCVcc, we found that W420Y retained 5% infectivity compared to wild type and the rest of the W420 mutants were non-infectious in the HCVpp system (Fig. 2a). The HCVpp infectivity data do not correspond to the E2-CD81 binding data (see below and Fig. 5a), as the W420F mutant retained CD81 binding activity but was not infectious. Thus, the reasons for the lower infectivity of the mutant HCVpps are not clear. Using E2 GNA-capture ELISA, we confirmed that the wild type and the mutant E2 glycoproteins were expressed intracellularly in comparable quantities (data not shown). However, we

consistently found less incorporation of E2 mutants W420A, W420V and W420R into the secreted HCVpps (Fig. 2b). The level of W420R E2 was extremely low while the levels of W420A and W420V mutant E2 were clearly reduced relative to wild type. In contrast, the incorporation of W420F and W420Y E2 into HCVpp was higher than that of the wild type protein even though the HCVpps displayed reduced or no infectivity in Huh7 cells (Fig. 2). The lack of infectivity of the W420A, V and R HCVpp mutants is likely explained by the reduced E2 incorporation into the pseudoparticles.

E2 mutations alter sensitivity to neutralizing antibodies. We assessed the reactivity of three broadly neutralizing monoclonal antibodies (mAbs), AP33, 3/11 and CBH-5 to each mutant E2 by GNA capture ELISA. Both AP33 and 3/11 bind to distinct but overlapping epitopes within the highly conserved region of E2 spanning residues 412 to 423 (QLINTNGSWHIN), with W420 being a critical contact residue for both antibodies (34). Recent structural data however, has revealed that this region is flexible. AP33 binds to a β-hairpin structure, in contrast, 3/11 recognizes an open conformation of this region (37-39). HmAb CBH-5 binds to an epitope within the CD81 binding region; substitution of E2 residues G523, P525, G530, D535 and N540 with alanine was reported to ablate CBH-5 binding, whereas mutation at W420 did not reduce binding by >50% (56). Further studies have shown that this antibody maps to immunodomain B and directly competes with CD81 for binding to E2 (44, 57, 58). A panel of HEK-293T cell lysates containing wild type or mutant HCV E1E2 was first tested for reactivity to an anti-E2 mAb DAO5 that recognizes a linear epitope spanning aa 532-540 (Vasiliauskaite *et al*. manuscript in preparation). As expected all lysates had similar reactivity to this mAb indicating that the proteins were expressed

372 in equivalent quantities (Fig. 3a). All W420 mutants showed undetectable binding
373 levels to mAb AP33 in the ELISA assay, confirming that this is a critical residue for
374 mAb AP33-E2 interaction (Fig. 3b). In contrast, while mutants W420A, V and R had
375 no detectable binding to mAb 3/11, both aromatic substitution mutants W420F and
376 W420Y retained 50% and 75% binding activity, respectively (Fig. 3c). The same
377 panel of lysates was assessed for reactivity with HmAb CBH-5, which binds a
378 conformational epitope within antigenic domain B of E2 (47). Although all W420
379 mutants retained some level of binding activity, this correlated with the type of
380 residue substituted. Both aromatic mutants (W420F and W420Y) retained 55% of
381 binding activity compared to wild type, and both aliphatic residues (W420A and
382 W420V) had similar binding, 36% and 41% of wild type respectively, while E2
383 containing the positively charged W420R substitution only bound HmAb CBH-5 at
384 20% of wild type activity. Subsequently, we investigated if these antibodies could
385 neutralize W420 mutant virus, using the two aromatic mutants, which had similar
386 levels of infectivity to wild type JFH-1. We found as predicted by the ELISA E2-
387 binding assay results that JFH-1_{W420Y} was completely resistant to neutralization by
388 mAb AP33. Surprisingly, JFH-1_{W420F} showed a low but consistent level of inhibition
389 at the highest concentrations of AP33 antibody tested (Fig. 4a) suggesting that this
390 mutant can still bind mAb AP33 albeit at a level undetectable by ELISA assay. In
391 contrast, we found that both mutants were neutralized by the 3/11 antibody that binds
392 to $E2_{412-423}$ in the open conformation. Although JFH-1_{W420F} only binds mAb 3/11 to
393 approximately 50% wild type levels, the inhibition profile did not show a
394 corresponding change. Instead the mutant virus was inhibited similarly to wild type
395 JFH-1 despite the reduction in binding affinity. Indeed the JFH-1_{W420Y} mutant that
396 retained 75% binding activity was found to be more sensitive to neutralization by

mAb 3/11 than wild type virus (Fig. 4b). We also tested neutralization using the CBH-5 antibody that binds to an epitope within the CD81 binding region of E2 (Fig. 4c). Notably, both mutants were significantly more sensitive to inhibition with this antibody, with approximately 2000-fold less antibody required to inhibit the mutant viruses by 50% compared to wild type virus. The differences observed between the sensitivity of these mutant viruses to neutralization by these human and rodent antibodies versus their glycoprotein reactivity by ELISA indicates that the mutations may enhance the exposure of E2 on the virion.

E2 mutations alter virus-receptor interactions. We used the panel of W420 E1E2 lysates to examine the E2-CD81 binding reactivity of the intracellular viral glycoproteins to sCD81-LEL by ELISA. Remarkably, the majority of 420 mutants had no detectable binding to CD81, confirming the importance of this residue in the E2-CD81 interaction (Fig. 5a). The JFH-1_{W420F} mutant however, could still bind to sCD81-LEL although binding was approximately 40% of wild type levels. To determine if the mutations have also reduced the affinity of E2 on the virion for the virus receptor CD81 we monitored neutralization of the JFH-1_{WT}, JFH-1_{W420F} and JFH-1_{W420Y} viruses. Firstly, we used an anti-CD81 neutralizing antibody that binds to the CD81 receptor on the cell surface, and found that all viruses were similarly inhibited irrespective of their ability to bind sCD81-LEL in the ELISA assay (Fig. 5b). Secondly, a competition assay using sCD81-LEL was performed. In this experiment we found that both W420 mutants were more sensitive to inhibition than JFH-1_{WT}, with JFH-1_{W420F} being the most sensitive (Fig. 5c). Even though no E2-CD81 interaction was detected in the ELISA assay for the JFH-1_{W420Y}, the inhibition profile with sCD81-LEL indicates that this mutant retains some affinity to CD81. This

parallels the earlier observations with mAb AP33 (Figs. 3b and 4a). Notably, the sensitivity of the mutant viruses to inhibition by sCD81-LEL (Fig. 5c) would not be predicted by their CD81-binding activity (Fig. 5a) although W420F that retained 40% binding activity to sCD81-LEL was the most sensitive to inhibition. This is in line with their greatly increased sensitivity to neutralization by HmAb CBH-5 (Fig. 4c), despite weaker binding to CBH-5 in ELISA (Fig. 3d). Together these data suggest increased exposure of CD81-binding sites on the 420 mutant virions.

Having established that these mutations influence the HCV-CD81 interaction, we investigated their effects on SR-BI-dependent entry. SR-BI has been reported to have three distinct functions in HCV entry; modulating primary attachment via interaction with apolipoproteins such as ApoE on the HCV virion, an access function that depends on the lipid transfer activity of SR-BI and finally an infectivity enhancement function (30). Only the latter function is thought to require E2-SR-BI interaction. To investigate whether mutation at position 420 alters the interaction of the virion with the SR-BI receptor we monitored SR-BI neutralization of the JFH-1_{WT}, JFH-1_{W420F} and JFH-1_{W420Y} viruses. The human-mouse anti-SR-BI mAb151-NP1 was expressed and purified, then specificity for human SR-BI was confirmed. The ability of anti-SR-BI mAb151-NP1 to bind to CHO-KI cells expressing human SR-BI or human SR-BI.EGFP was assessed by FACS analysis. Firstly, detection of GFP in the CHO-hSR-BI-GFP cells confirmed expression of the SR-BI-EGFP fusion protein (Fig.6a). As expected anti-SR-BI mAb151-NP1 bound to CHO-K1 cells expressing human SR-BI or human SR-BI.EGFP but not to the parental CHO-K1 cell-line confirming that the antibody specifically recognizes human SR-BI (Fig.6b, 6c, 6d). Naive Huh7-J20 cells were pre-incubated with varying concentrations of a neutralizing human-mouse anti-

447 SR-BI mAb151-NP1 prior to infection with each virus. Interestingly, both mutants
448 were considerably less sensitive than wild type to neutralization suggesting that these
449 mutants are significantly less dependent on SR-BI for virus entry (Fig. 6e). However,
450 the 420 mutants were inhibited by the highest concentrations of anti-SR-BI tested.
451 Inhibitory SR-BI antibodies have been shown to inhibit both the primary attachment
452 and lipid transfer activity functions (30). Therefore, to investigate which SR-BI
453 function targeted by antibody treatment was responsible for the reduced sensitivity;
454 we used the chemical inhibitor BLT-4 that blocks SR-BI lipid transfer activity (59).
455 Huh7-J20 cells were preincubated with increasing concentrations of BLT-4 before
456 infection with virus. In parallel, cell viability in the presence of BLT-4 was assessed
457 and found to not be affected (Fig. 6g). JFH-1_{WT} virus was sensitive to BLT-4
458 treatment; in contrast the JFH-1_{W420F} and JFH-1_{W420Y} viruses were not inhibited even
459 at the highest dose (Fig.6f). These data suggest that the W420 mutant viruses access
460 the cells independently of SR-BI lipid transfer activity but can still use SR-BI for
461 primary attachment.
462
463 Studies have shown that high density lipoprotein (HDL) enhances HCVcc entry via
464 SR-BI (60, 61). More recently Diao *et al* (2012) demonstrate that HDL enhancement
465 can be inhibited by treatment with erlotinib that targets EGFR, a known host factor for
466 HCV entry (62). This indicates that SR-BI and EGFR may use the same
467 internalization pathway. Therefore we investigated whether mutation of W420
468 affected EGFR-dependent entry. Naïve cells were pretreated with the EGFR kinase
469 inhibitor erlotinib prior to infection with virus. As expected JFH-1_{WT} virus was
470 sensitive to erlotinib in a dose-dependent manner with an IC_{50} of 0.244μM, which is
471 in agreement with the range observed previously (Fig. 7a) (23, 62). In comparison the

JFH-1_{W420F} and JFH-1_{W420Y} viruses were markedly less sensitive to erlotinib treatment. In parallel, cell viability was assessed and erlotinib treatment was found to have no effect (Fig.7b). Erlotinib targets the tyrosine kinase domain of EGFR; however previous studies also indicate a role for the ligand-binding domain of EGFR in HCV entry. Although the previous studies agree that EGFR ligands such as EGF promote HCV infection, the data is conflicting with regard to the effect of an EGFR neutralizing antibody that prevents ligand interaction (23, 62). We determined the response of JFH-1_{WT}, JFH-1_{W420F} or JFH-1_{W420Y} to incubation in the presence of EGFR antibody (LA-1) (Fig.7c). In agreement with Diao and co-workers we found that antibody treatment did not block JFH-1_{WT} HCVcc infection. Moreover, there was no difference between the wildtype virus and the W420 mutants. The main target of erlotinib is EGFR however; Neveu *et al* recently reported that erlotinib also inhibits cyclin G-associated kinase (GAK) during HCV entry (63). GAK is a regulator of clathrin-mediated endocytosis that recruits clathrin and AP2 to the plasma membrane. GAK has been shown to regulate EGFR internalization and promote EGF uptake (64). Therefore erlotinib treatment targets two steps of the EGFR pathway. The resistance to erlotinib inhibition indicates that JFH-1_{W420F} and JFH-1_{W420Y} do not require the EGFR/GAK route for entry. The host cell kinase AP-2-associated protein kinase 1 (AAK1) is a second regulator of AP-2 clathrin-mediated endocytosis. AAK1 was also shown to regulate EGFR-mediated HCV entry (63). Therefore we used sunitinib, a kinase inhibitor that targets AAK1 to investigate if the W420 mutants require AAK1. Huh7-J20 cells were pretreated with increasing concentrations of sunitinib prior to infection with virus. We found that JFH-1_{WT}, JFH-1_{W420F} and JFH-1_{W420Y} viruses were inhibited by sunitinib in a dose-dependent manner (Fig.7d). Interestingly, at the highest concentrations tested the mutants were more sensitive to sunitinib inhibition

497 than JFH-1_{WT} virus indicating that the mutants were more dependent on this entry
498 route (Fig.7e). Sunitinib treatment was found to only affect cell viability at the highest
499 concentration tested (Fig.7f).
500
501 **DISCUSSION**
502 We investigated the role of the highly conserved tryptophan at aa position 420 within
503 the AP33 epitope of the E2 glycoprotein by substituting this residue in the full length
504 viral genome with phenylalanine, tyrosine, alanine, arginine and valine. The
505 phenotypes of the E2 mutants in this study highlight the importance of tryptophan 420
506 during virus infection. None of the substitutions at position 420 had an effect on viral
507 replication levels, but overall viral titers of the JFH-1_{W420A} and JFH-1_{W420R} viruses
508 were significantly decreased. Analysis of the amount of HCV core protein present in
509 the medium indicates that there is no effect on virus assembly and secretion. The
510 decrease in viral titers is apparent in the FFU/ml assay, which requires infection of
511 naïve cells, and therefore reveals a defect in the entry step of the viral lifecycle.
512
513 It is remarkable that the only mutation at this position detected in one out of 2161
514 naturally occurring HCV sequences was W420R, particularly as our results indicate
515 that this virus is very disabled. In addition, the fact that upon serial passaging, the
516 JFH-1_{W420R} virus reverted to the wild type sequence is strong evidence that W420 is
517 important for function. However, these mutations were only assessed in a JFH-1
518 background, therefore it is possible that other compensatory mutations were present in
519 the natural variant that improved viral fitness. In terms of amino acid properties,
520 phenylalanine and tyrosine are the most conservative mutations to replace tryptophan.
521 Indeed, the unaltered infectivity of the JFH-1_{W420F} and JFH-1_{W420Y} mutants suggest

522 that other aromatic residues can replace the tryptophan residue at this position.
523 Furthermore, our results with JFH-1_{W420A} and JFH-1_{W420V} also demonstrate that
524 smaller residues can substitute for the tryptophan, albeit less efficiently in the case of
525 alanine. Indeed considering our mutagenesis data in the HCVcc system it is somewhat
526 surprising that W420 is so strictly conserved in nature. In contrast, the data from the
527 HCVpp system clearly show that tryptophan is essential at this position as all
528 substitutions severely reduced infectivity. Our data also suggest a requirement for
529 W420 for efficient assembly of HCVpps, as W420A, V and R HCVpp contained low
530 levels of E2 glycoprotein. Further analysis would be required to assess if a similar
531 defect is observed in the HCVcc system, although this is unlikely to be the case at
532 least with the JFH-1_{W420V} mutant, which exhibited infectivity levels that were similar
533 to those of the wild type HCVcc (Fig. 1d).
534
535 At first glance, a comparison of the data for binding and for neutralization by the E2
536 conformational antibody HmAb CBH-5 or by sCD81-LEL shows a lack of direct
537 correlation between the two properties. This is in concordance with observations in
538 other virus systems, as neutralization activity is dependent on many additional factors
539 (65-67). Our assays showed that the mutant E2 glycoproteins bound more weakly than
540 the wild type to HmAb CBH-5 or sCD81-LEL, whereas the corresponding mutant
541 virions were more sensitive than wild type virus to neutralization by these same
542 molecules suggesting a clear difference between the wild type and mutant virions.
543 There are numerous possible mechanisms that may influence sensitivity to
544 neutralization. These include differences in binding affinity between wild type and
545 mutant E2, the number of functional E1E2 complexes present on the virion surface
546 and the number of antibody or receptor molecules required to neutralize. For example

547 a change in angle of the antibody relative to the virion surface will affect the amount
548 of steric hindrance caused by a single molecule. The HCV virion is protected by a
549 glycan shield (68), therefore it is possible that mutation of W420 affects the position
550 of the glycans and increases exposure of the antibody epitope. However, in the core
551 E2 structure, the majority of glycans were positioned on a different face of E2 and the
552 CD81/CBH-5 binding site was relatively exposed, suggesting that this is not a likely
553 explanation (35). There is evidence that this region is masked by HVR1 (69-71) in the
554 native virions. During virus entry interaction with a host factor induces a
555 conformational change exposing the CD81-binding site and enabling interaction with
556 CD81. Both wild type and mutant viruses were similarly neutralized by anti-CD81,
557 which prevents virion-CD81 interaction by blocking CD81 receptors on the cell,
558 indicating that substitution at position 420 did not alter CD81-dependence of
559 infectivity. This demonstrates that there was no significant net decrease in virion-
560 CD81 interaction despite the decreased affinity for CD81, suggesting that this was
561 counteracted by improved accessibility of the CD81-binding region. Indeed, the
562 increased sensitivity to competition with sCD81-LEL indicates that the CD81-binding
563 region on the mutant virion is more exposed than on the wild type virion. This
564 observation is analogous to an earlier study of viruses with point mutations within this
565 region. E1E2 containing the mutations N415D, T416A, N417S and I422L bound
566 sCD81-LEL similarly or better than wild type (53). This is in contrast to E1E2
567 containing mutations at position 420 that had reduced or undetectable levels of
568 binding compared to wild type E1E2 supporting the hypothesis that tryptophan 420 is
569 important for E2-CD81 interaction. The fact that the reduced affinity for E1E2 does
570 not appear to have a detrimental effect on virion-CD81 interaction demonstrates either
571 that increased exposure of CD81-binding sites on the virion can compensate

572 completely or that the affinity of E1E2 on the virion is not as strongly reduced by
573 mutations at this position.
574
575 The neutralization experiment with anti-SR-BI found that substitution of W420
576 reduced the requirement for SR-BI for infectivity of these viruses. Again, this is
577 consistent with several studies of viruses with mutations within this region. Viruses
578 containing the point mutations I414T, N415D, T416A, N417S and I422L in E2 were
579 all shown to have reduced sensitivity to inhibition by anti-SR-BI (53, 72). The HVR1
580 region of E2 lies immediately upstream and virus with a complete deletion of HVR1
581 (delHVR1) was shown to be completely resistant to neutralization by anti-SR-BI (69).
582 The delHVR1 result was expected as several studies have shown that E2-SR-BI
583 interaction maps to HVR1 and more recently that inhibition by anti-SR-BI or SR-BI
584 inhibitors maps to this region (19, 69, 70). However, HVR1 is still present in the
585 W420 mutants suggesting that the SR-BI binding site is less accessible in the mutant
586 virions. The complete resistance of the W420 mutant viruses to the inhibitor BLT-4
587 indicates that the reduced dependence on SR-BI is linked to the lipid transfer function
588 which is required for both the access and enhancement functions of SR-BI. This is
589 consistent with previous observations of mutant viruses N415D, T416A, N417S and
590 I422L that were resistant to HDL-mediated enhancement, which requires the SR-BI
591 lipid transfer activity (53, 73, 74). The observation that substitution of tryptophan 420
592 also rendered the viruses resistant to erlotinib that targets EGFR and GAK, two
593 components required for EGFR internalization suggests that the 420 mutant viruses do
594 not use this route for entry. The reduced dependence on SR-BI together with the
595 observation by Diao *et al* that erlotinib can also block SR-BI dependent HDL-
596 mediated enhancement strongly suggests that SR-BI, EGFR and GAK are involved in

597 the same entry route. The small but significant increase in sensitivity to sunitinib
598 indicates that substitution at position 420 makes the virus more reliant on AAK1-
599 dependent internalization. Therefore, together with the CD81 data, this indicates a
600 model where alteration at position 420 causes a subtle change in conformation or
601 flexibility of HVR1 that prevents interaction with SR-BI and increases accessibility to
602 the CD81 binding site. This in turn alters the entry requirements for clathrin-mediated
603 uptake blocking the SR-BI, EGFR, GAK pathway and favoring the CD81, EGFR,
604 AAK-1 route.
605
606 Two of the antibodies tested (AP33 and 3/11) bind to $E2_{412-423}$ and W420 has been
607 identified as a critical binding residue for both antibodies by alanine scanning and
608 structural analysis of antibody bound to peptide (34, 37-39). $E2_{412-423}$ is structurally
609 flexible and is recognized by each antibody in a different conformation. It adopts a β-
610 hairpin conformation when bound to mAb AP33 and a completely different linear,
611 open conformation when bound to mAb 3/11. Our data suggest that W420 is less
612 critical for interaction with mAb 3/11 as both hydrophobic substitutions retained
613 binding activity for mAb 3/11. Scrutiny of the antigen/antibody interfaces reveals that
614 the interaction of the W420 side chain with both antibodies is dominated 1) by
615 hydrophobic interactions and 2) by hydrogen bonds of the NE1 atom with the
616 carbonyl oxygens of T96 and T97 (mAb 3/11) or N91 (mAb AP33) of the light chain
617 (Fig. 8). The spatial organization of the two antigen/antibody complexes is such that
618 the distance between a hydrophobic phenyl ring as part of a phenylalanine or tyrosine
619 side chain in position 420 and the respective carbonyl oxygens would be shorter for
620 the AP33 complex (~2.7Å) than for the 3/11 complex (~3.2Å). This disadvantageous
621 interaction could explain the observed lower tolerance of mAb AP33 for a

622 phenylalanine or tyrosine residue at this position. Nevertheless, a hydrophobic residue
623 at this position is essential as all other mutations ablated binding activity.
624
625 Inspection of the neutralization profile of sCD81-LEL shows that JFH-1_{W420F} virus is
626 more sensitive to neutralization than JFH-1_{W420Y}, suggesting that the hydroxyl group
627 of the tyrosine side chain does not favor interaction with CD81. This is in line with
628 the fact that only the JFH-1_{W420F} mutant and not the JFH-1_{W420Y} mutant partially
629 retained CD81 binding activity and suggests that a polar group within the side chain
630 of residue 420 is not beneficial for receptor binding. One possible interpretation of
631 these results could be that this residue provides an additional hydrophobic anchor
632 point to bind the mostly hydrophobic binding site within CD81 (75). Of note, a
633 second antigenic region contributing to the CD81 binding site displays a hydrophobic
634 protrusion constituted by F442 and Y443 that is essential for virus propagation (76).
635 In conjunction with the conformational flexibility around W420 and the essential role
636 of a hydrophobic side chain at position 420 this suggests a stabilizing role of W420 in
637 E2-CD81 binding.
638
639 The aim of the present study was to determine if the E2 residue W420 was indeed a
640 contact residue for the CD81 receptor during HCVcc entry. Our results clearly show
641 that W420 is required for virus entry and is required for E2-CD81 binding in the
642 virion. In addition, our data highlights the relationship between E2-CD81 and E2-SR-
643 BI interaction as mutation at this position also modulates the interaction of the virion
644 with the SR-BI receptor and the subsequent internalization route. The strong
645 requirement for a hydrophobic residue at position 420 also provides new insights into
646 the mode of binding to the cellular receptor.

FUNDING INFORMATION

This work was supported by the UK Medical Research Council-funded grant (MC_UU_12014/2) to AHP. Thomas Krey acknowledges financial support by the ANRS.

ACKNOWLEDGEMENTS

We thank Steven Foung, Jane McKeating and Charles Rice for the kind gifts of antibodies used in this study and Takaji Wakita for the JFH-1 HCVcc cDNA constructs.

REFERENCES

1. **Simmonds P.** 2004. Genetic diversity and evolution of hepatitis C virus--15 years on. J Gen Virol **85:**3173-3188.
2. **Tellinghuisen TL, Evans MJ, von Hahn T, You S, Rice CM.** 2007. Studying hepatitis C virus: making the best of a bad virus. J Virol **81:**8853-8867.
3. **Bartenschlager R, Penin F, Lohmann V, Andre P.** 2011. Assembly of infectious hepatitis C virus particles. Trends Microbiol **19:**95-103.
4. **Jones CT, Murray CL, Eastman DK, Tassello J, Rice CM.** 2007. Hepatitis C virus p7 and NS2 proteins are essential for production of infectious virus. J Virol **81:**8374-8383.
5. **de la Fuente C, Goodman Z, Rice CM.** 2013. Genetic and functional characterization of the N-terminal region of the hepatitis C virus NS2 protein. J Virol **87:**4130-4145.

6. **Wozniak AL, Griffin S, Rowlands D, Harris M, Yi M, Lemon SM, Weinman SA.** 2010. Intracellular proton conductance of the hepatitis C virus p7 protein and its contribution to infectious virus production. PLoS Pathog **6:**e1001087. doi:10:1371/journal.ppat.1001087

7. **Lohmann V.** 2013. Hepatitis C virus RNA replication. Curr Top Microbiol Immunol **369:**167-198.

8. **Smith DB, Bukh J, Kuiken C, Muerhoff AS, Rice CM, Stapleton JT, Simmonds P.** 2014. Expanded classification of hepatitis C virus into 7 genotypes and 67 subtypes: updated criteria and genotype assignment web resource. Hepatology **59:**318-327.

9. **Neumann AU, Lam NP, Dahari H, Gretch DR, Wiley TE, Layden TJ, Perelson AS.** 1998. Hepatitis C viral dynamics in vivo and the antiviral efficacy of interferon-alpha therapy. Science **282:**103-107.

10. **Troesch M, Meunier I, Lapierre P, Lapointe N, Alvarez F, Boucher M, Soudeyns H.** 2006. Study of a novel hypervariable region in hepatitis C virus (HCV) E2 envelope glycoprotein. Virology **352:**357-367.

11. **Nielsen SU, Bassendine MF, Burt AD, Martin C, Pumeechockchai W, Toms GL.** 2006. Association between hepatitis C virus and very-low-density lipoprotein (VLDL)/LDL analyzed in iodixanol density gradients. J Virol **80:**2418-2428.

12. **Felmlee DJ, Hafirassou ML, Lefevre M, Baumert TF, Schuster C.** 2013. Hepatitis C virus, cholesterol and lipoproteins--impact for the viral life cycle and pathogenesis of liver disease. Viruses **5:**1292-1324.

13. **Chang KS, Jiang J, Cai Z, Luo G.** 2007. Human apolipoprotein e is required for infectivity and production of hepatitis C virus in cell culture. J Virol **81:**13783-13793.

14. **Agnello V, Abel G, Elfahal M, Knight GB, Zhang QX.** 1999. Hepatitis C virus and other flaviviridae viruses enter cells via low density lipoprotein receptor. Proc Natl Acad Sci U S A **96:**12766-12771.

15. **Barth H, Schnober EK, Zhang F, Linhardt RJ, Depla E, Boson B, Cosset FL, Patel AH, Blum HE, Baumert TF.** 2006. Viral and cellular determinants of the hepatitis C virus envelope-heparan sulfate interaction. J Virol **80:**10579-10590.

16. **Jiang J, Cun W, Wu X, Shi Q, Tang H, Luo G.** 2012. Hepatitis C virus attachment mediated by apolipoprotein E binding to cell surface heparan sulfate. J Virol **86:**7256-7267.

17. **Jiang J, Wu X, Tang H, Luo G.** 2013. Apolipoprotein E mediates attachment of clinical hepatitis C virus to hepatocytes by binding to cell surface heparan sulfate proteoglycan receptors. PloS One **8:**e67982. doi:10.1371/journal.pone.0067982

18. **Owen DM, Huang H, Ye J, Gale M, Jr.** 2009. Apolipoprotein E on hepatitis C virion facilitates infection through interaction with low-density lipoprotein receptor. Virology **394:**99-108.

19. **Scarselli E, Ansuini H, Cerino R, Roccasecca RM, Acali S, Filocamo G, Traboni C, Nicosia A, Cortese R, Vitelli A.** 2002. The human scavenger receptor class B type I is a novel candidate receptor for the hepatitis C virus. EMBO J **21:**5017-5025.

20. **Pileri P, Uematsu Y, Campagnoli S, Galli G, Falugi F, Petracca R, Weiner AJ, Houghton M, Rosa D, Grandi G, Abrignani S.** 1998. Binding of hepatitis C virus to CD81. Science **282:**938-941.

21. **Evans MJ, von Hahn T, Tscherne DM, Syder AJ, Panis M, Wolk B, Hatziioannou T, McKeating JA, Bieniasz PD, Rice CM.** 2007. Claudin-1 is a hepatitis C virus co-receptor required for a late step in entry. Nature **446:**801-805.

22. **Ploss A, Evans MJ, Gaysinskaya VA, Panis M, You H, de Jong YP, Rice CM.** 2009. Human occludin is a hepatitis C virus entry factor required for infection of mouse cells. Nature **457:**882-886.

23. **Lupberger J, Zeisel MB, Xiao F, Thumann C, Fofana I, Zona L, Davis C, Mee CJ, Turek M, Gorke S, Royer C, Fischer B, Zahid MN, Lavillette D, Fresquet J, Cosset FL, Rothenberg SM, Pietschmann T, Patel AH, Pessaux P, Doffoel M, Raffelsberger W, Poch O, McKeating JA, Brino L, Baumert TF.** 2011. EGFR and EphA2 are host factors for hepatitis C virus entry and possible targets for antiviral therapy. Nat Med **17:**589-595.

24. **Zona L, Lupberger J, Sidahmed-Adrar N, Thumann C, Harris HJ, Barnes A, Florentin J, Tawar RG, Xiao F, Turek M, Durand SC, Duong FH, Heim MH, Cosset FL, Hirsch I, Samuel D, Brino L, Zeisel MB, Le Naour F, McKeating JA, Baumert TF.** 2013. HRas signal transduction promotes hepatitis C virus cell entry by triggering assembly of the host tetraspanin receptor complex. Cell Host Microbe **13:**302-313.

25. **Sainz B, Jr., Barretto N, Martin DN, Hiraga N, Imamura M, Hussain S, Marsh KA, Yu X, Chayama K, Alrefai WA, Uprichard SL.** 2012.

Identification of the Niemann-Pick C1-like 1 cholesterol absorption receptor as a new hepatitis C virus entry factor. Nat Med **18:**281-285.

26. **Martin DN, Uprichard SL.** 2013. Identification of transferrin receptor 1 as a hepatitis C virus entry factor. Proc Natl Acad Sci U S A **110:**10777-10782.

27. **Blanchard E, Belouzard S, Goueslain L, Wakita T, Dubuisson J, Wychowski C, Rouille Y.** 2006. Hepatitis C virus entry depends on clathrin-mediated endocytosis. J Virol **80:**6964-6972.

28. **Meertens L, Bertaux C, Dragic T.** 2006. Hepatitis C virus entry requires a critical postinternalization step and delivery to early endosomes via clathrin-coated vesicles. J Virol **80:**11571-11578.

29. **Tscherne DM, Jones CT, Evans MJ, Lindenbach BD, McKeating JA, Rice CM.** 2006. Time- and temperature-dependent activation of hepatitis C virus for low-pH-triggered entry. J Virol **80:**1734-1741.

30. **Dao Thi VL, Granier C, Zeisel MB, Guerin M, Mancip J, Granio O, Penin F, Lavillette D, Bartenschlager R, Baumert TF, Cosset FL, Dreux M.** 2012. Characterization of hepatitis C virus particle subpopulations reveals multiple usage of the scavenger receptor BI for entry steps. J Biol Chem **287:**31242-31257.

31. **Feneant L, Levy S, Cocquerel L.** 2014. CD81 and hepatitis C virus (HCV) infection. Viruses **6:**535-572.

32. **Vieyres G, Thomas X, Descamps V, Duverlie G, Patel AH, Dubuisson J.** 2010. Characterization of the envelope glycoproteins associated with infectious hepatitis C virus. J Virol **84:**10159-10168.

33. **Owsianka AM, Timms JM, Tarr AW, Brown RJ, Hickling TP, Szwejk A, Bienkowska-Szewczyk K, Thomson BJ, Patel AH, Ball JK.** 2006. Identification of conserved residues in the E2 envelope glycoprotein of the hepatitis C virus that are critical for CD81 binding. J Virol **80:**8695-8704.

34. **Tarr AW, Owsianka AM, Timms JM, McClure CP, Brown RJ, Hickling TP, Pietschmann T, Bartenschlager R, Patel AH, Ball JK.** 2006. Characterization of the hepatitis C virus E2 epitope defined by the broadly neutralizing monoclonal antibody AP33. Hepatology **43:**592-601.

35. **Kong L, Giang E, Robbins JB, Stanfield RL, Burton DR, Wilson IA, Law M.** 2012. Structural basis of hepatitis C virus neutralization by broadly neutralizing antibody HCV1. Proc Natl Acad Sci U S A **109:**9499-9504.

36. **Angus AGN, Patel AH.** 2011. Immunotherapeutic potential of neutralizing antibodies targeting conserved regions of the HCV envelope glycoprotein E2 (vol 6, pg 279, 2011). Future Microbiol **6:**600-600.

37. **Potter JA, Owsianka AM, Jeffery N, Matthews DJ, Keck ZY, Lau P, Foung SK, Taylor GL, Patel AH.** 2012. Toward a hepatitis C virus vaccine: the structural basis of hepatitis C virus neutralization by AP33, a broadly neutralizing antibody. J Virol **86:**12923-12932.

38. **Kong L, Giang E, Nieusma T, Robbins JB, Deller MC, Stanfield RL, Wilson IA, Law M.** 2012. Structure of hepatitis C virus envelope glycoprotein E2 antigenic site 412 to 423 in complex with antibody AP33. J Virol **86:**13085-13088.

39. **Meola A, Tarr AW, England P, Meredith LW, McClure CP, Foung SK, McKeating JA, Ball JK, Rey FA, Krey T.** 2015. Structural flexibility of a

conserved antigenic region in hepatitis C virus glycoprotein E2 recognized by broadly neutralizing antibodies. J Virol **89:**2170-2181.

40. **Pantua H, Diao J, Ultsch M, Hazen M, Mathieu M, McCutcheon K, Takeda K, Date S, Cheung TK, Phung Q, Hass P, Arnott D, Hongo JA, Matthews DJ, Brown A, Patel AH, Kelley RF, Eigenbrot C, Kapadia SB.** 2013. Glycan shifting on hepatitis C virus (HCV) E2 glycoprotein is a mechanism for escape from broadly neutralizing antibodies. J Mol Biol **425:**1899-1914.

41. **Nakabayashi H, Taketa K, Miyano K, Yamane T, Sato J.** 1982. Growth of human hepatoma cells lines with differentiated functions in chemically defined medium. Cancer Res **42:**3858-3863.

42. **Iro M, Witteveldt J, Angus AG, Woerz I, Kaul A, Bartenschlager R, Patel AH.** 2009. A reporter cell line for rapid and sensitive evaluation of hepatitis C virus infectivity and replication. Antiviral Res **83:**148-155.

43. **Clayton RF, Owsianka A, Aitken J, Graham S, Bhella D, Patel AH.** 2002. Analysis of antigenicity and topology of E2 glycoprotein present on recombinant hepatitis C virus-like particles. J Virol **76:**7672-7682.

44. **Hadlock KG, Lanford RE, Perkins S, Rowe J, Yang Q, Levy S, Pileri P, Abrignani S, Foung SK.** 2000. Human monoclonal antibodies that inhibit binding of hepatitis C virus E2 protein to CD81 and recognize conserved conformational epitopes. J Virol **74:**10407-10416.

45. **Keck ZY, Op De Beeck A, Hadlock KG, Xia J, Li TK, Dubuisson J, Foung SK.** 2004. Hepatitis C virus E2 has three immunogenic domains containing conformational epitopes with distinct properties and biological functions. J Virol **78:**9224-9232.

46. **Flint M, Maidens C, Loomis-Price LD, Shotton C, Dubuisson J, Monk P, Higginbottom A, Levy S, McKeating JA.** 1999. Characterization of hepatitis C virus E2 glycoprotein interaction with a putative cellular receptor, CD81. J Virol **73:**6235-6244.

47. **Lindenbach BD, Evans MJ, Syder AJ, Wolk B, Tellinghuisen TL, Liu CC, Maruyama T, Hynes RO, Burton DR, McKeating JA, Rice CM.** 2005. Complete replication of hepatitis C virus in cell culture. Science **309:**623-626.

48. **Lacek K, Vercauteren K, Grzyb K, Naddeo M, Verhoye L, Slowikowski MP, Fafi-Kremer S, Patel AH, Baumert TF, Folgori A, Leroux-Roels G, Cortese R, Meuleman P, Nicosia A.** 2012. Novel human SR-BI antibodies prevent infection and dissemination of HCV in vitro and in humanized mice. J Hepatol **57:**17-23.

49. **Wakita T, Pietschmann T, Kato T, Date T, Miyamoto M, Zhao Z, Murthy K, Habermann A, Krausslich HG, Mizokami M, Bartenschlager R, Liang TJ.** 2005. Production of infectious hepatitis C virus in tissue culture from a cloned viral genome. Nat Med **11:**791-796.

50. **Witteveldt J, Evans MJ, Bitzegeio J, Koutsoudakis G, Owsianka AM, Angus AG, Keck ZY, Foung SK, Pietschmann T, Rice CM, Patel AH.** 2009. CD81 is dispensable for hepatitis C virus cell-to-cell transmission in hepatoma cells. J Gen Virol **90:**48-58.

51. **Zhong J, Gastaminza P, Cheng G, Kapadia S, Kato T, Burton DR, Wieland SF, Uprichard SL, Wakita T, Chisari FV.** 2005. Robust hepatitis C virus infection in vitro. Proc Natl Acad Sci U S A**102:**9294-9299.

52. **Gastaminza P, Kapadia SB, Chisari FV.** 2006. Differential biophysical properties of infectious intracellular and secreted hepatitis C virus particles. J Virol **80:**11074-11081.

53. **Dhillon S, Witteveldt J, Gatherer D, Owsianka AM, Zeisel MB, Zahid MN, Rychlowska M, Foung SK, Baumert TF, Angus AG, Patel AH.** 2010. Mutations within a conserved region of the hepatitis C virus E2 glycoprotein that influence virus-receptor interactions and sensitivity to neutralizing antibodies. J Virol **84:**5494-5507.

54. **Patel AH, Wood J, Penin F, Dubuisson J, McKeating JA.** 2000. Construction and characterization of chimeric hepatitis C virus E2 glycoproteins: analysis of regions critical for glycoprotein aggregation and CD81 binding. J Gen Virol **81:**2873-2883.

55. **Kitadokoro K, Bordo D, Galli G, Petracca R, Falugi F, Abrignani S, Grandi G, Bolognesi M.** 2001. CD81 extracellular domain 3D structure: insight into the tetraspanin superfamily structural motifs. EMBO J **20:**12-18.

56. **Owsianka AM, Tarr AW, Keck ZY, Li TK, Witteveldt J, Adair R, Foung SK, Ball JK, Patel AH.** 2008. Broadly neutralizing human monoclonal antibodies to the hepatitis C virus E2 glycoprotein. J Gen Virol **89:**653-659.

57. **Bailey JR, Wasilewski LN, Snider AE, El-Diwany R, Osburn WO, Keck Z, Foung SK, Ray SC.** 2015. Naturally selected hepatitis C virus polymorphisms confer broad neutralizing antibody resistance. J Clin Invest **125:**437-447.

58. **Keck ZY, Li TK, Xia J, Gal-Tanamy M, Olson O, Li SH, Patel AH, Ball JK, Lemon SM, Foung SK.** 2008. Definition of a conserved immunodominant domain on hepatitis C virus E2 glycoprotein by neutralizing human monoclonal antibodies. J Virol **82:**6061-6066.

59. **Nieland TJ, Penman M, Dori L, Krieger M, Kirchhausen T.** 2002. Discovery of chemical inhibitors of the selective transfer of lipids mediated by the HDL receptor SR-BI. Proc Natl Acad Sci U S A **99:**15422-15427.

60. **Dreux M, Pietschmann T, Granier C, Voisset C, Ricard-Blum S, Mangeot PE, Keck Z, Foung S, Vu-Dac N, Dubuisson J, Bartenschlager R, Lavillette D, Cosset FL.** 2006. High density lipoprotein inhibits hepatitis C virus-neutralizing antibodies by stimulating cell entry via activation of the scavenger receptor BI. J Biol Chem **281:**18285-18295.

61. **Zeisel MB, Koutsoudakis G, Schnober EK, Haberstroh A, Blum HE, Cosset FL, Wakita T, Jaeck D, Doffoel M, Royer C, Soulier E, Schvoerer E, Schuster C, Stoll-Keller F, Bartenschlager R, Pietschmann T, Barth H, Baumert TF.** 2007. Scavenger receptor class B type I is a key host factor for hepatitis C virus infection required for an entry step closely linked to CD81. Hepatology **46:**1722-1731.

62. **Diao J, Pantua H, Ngu H, Komuves L, Diehl L, Schaefer G, Kapadia SB.** 2012. Hepatitis C virus induces epidermal growth factor receptor activation via CD81 binding for viral internalization and entry. J Virol **86:**10935-10949.

63. **Neveu G, Ziv-Av A, Barouch-Bentov R, Berkerman E, Mulholland J, Einav S.** 2015. AP-2-associated protein kinase 1 and cyclin G-associated

kinase regulate hepatitis C virus entry and are potential drug targets. J Virol **89:**4387-4404.

64. **Lee DW, Zhao X, Zhang F, Eisenberg E, Greene LE.** 2005. Depletion of GAK/auxilin 2 inhibits receptor-mediated endocytosis and recruitment of both clathrin and clathrin adaptors. J Cell Sci **118:**4311-4321.

65. **Burton DR, Williamson RA, Parren PW.** 2000. Antibody and virus: binding and neutralization. Virology **270:**1-3.

66. **Klasse PJ, Sattentau QJ.** 2002. Occupancy and mechanism in antibody-mediated neutralization of animal viruses. J Gen Virol **83:**2091-2108.

67. **Reading SA, Dimmock NJ.** 2007. Neutralization of animal virus infectivity by antibody. Arch Virol **152:**1047-1059.

68. **Helle F, Duverlie G, Dubuisson J.** 2011. The hepatitis C virus glycan shield and evasion of the humoral immune response. Viruses **3:**1909-1932.

69. **Bankwitz D, Steinmann E, Bitzegeio J, Ciesek S, Friesland M, Herrmann E, Zeisel MB, Baumert TF, Keck ZY, Foung SK, Pecheur EI, Pietschmann T.** 2010. Hepatitis C virus hypervariable region 1 modulates receptor interactions, conceals the CD81 binding site, and protects conserved neutralizing epitopes. J Virol **84:**5751-5763.

70. **Bankwitz D, Vieyres G, Hueging K, Bitzegeio J, Doepke M, Chhatwal P, Haid S, Catanese MT, Zeisel MB, Nicosia A, Baumert TF, Kaderali L, Pietschmann T.** 2014. Role of hypervariable region 1 for the interplay of hepatitis C virus with entry factors and lipoproteins. J Virol **88:**12644-12655.

71. **Roccasecca R, Ansuini H, Vitelli A, Meola A, Scarselli E, Acali S, Pezzanera M, Ercole BB, McKeating J, Yagnik A, Lahm A, Tramontano A, Cortese R, Nicosia A.** 2003. Binding of the hepatitis C virus E2 glycoprotein to CD81 is strain specific and is modulated by a complex interplay between hypervariable regions 1 and 2. J Virol **77:**1856-1867.

72. **Tao WY, Xu CL, Ding Q, Li R, Xiang Y, Chung J, Zhong J.** 2009. A single point mutation in E2 enhances hepatitis C virus infectivity and alters lipoprotein association of viral particles. Virology **395:**67-76.

73. **Dreux M, Dao Thi VL, Fresquet J, Guerin M, Julia Z, Verney G, Durantel D, Zoulim F, Lavillette D, Cosset FL, Bartosch B.** 2009. Receptor complementation and mutagenesis reveal SR-BI as an essential HCV entry factor and functionally imply its intra- and extra-cellular domains. PLoS Pathog **5:**e1000310. doi:10.1371/journal.ppat.1000310

74. **Voisset C, Callens N, Blanchard E, Op De Beeck A, Dubuisson J, Vu-Dac N.** 2005. High density lipoproteins facilitate hepatitis C virus entry through the scavenger receptor class B type I. J Biol Chem **280:**7793-7799.

75. **Drummer HE, Wilson KA, Poumbourios P.** 2002. Identification of the hepatitis C virus E2 glycoprotein binding site on the large extracellular loop of CD81. J Virol **76:**11143-11147.

76. **Krey T, Meola A, Keck ZY, Damier-Piolle L, Foung SK, Rey FA.** 2013. Structural basis of HCV neutralization by human monoclonal antibodies resistant to viral neutralization escape. PLoS Pathog **9:**e1003364. doi:10.1371/journal.ppat.1003364

939 **FIGURE LEGENDS**

940 **Figure 1. Analysis of W420 mutant viruses.** Huh7 cells were transfected with viral
941 RNA transcribed from cDNA encoding JFH-1_{WT}, JFH-1_{GND}, JFH-1_{DE1E2} and a panel
942 of JFH-1_{W420} mutants and analyzed after 72h. (a) Intracellular viral replication was
943 quantified by SEAP activity (RLU). (b) Viral titers were quantified by FFU/ml assay;
944 black bars show extracellular virus harvested from the medium, grey bars show
945 intracellular virus harvested from lysed cells. (c) Western blot analysis to detect (i)
946 viral proteins Core, E2, NS5A and tubulin loading control in mock-infected (MI) and
947 infected cell lysates and (ii) Core protein in released virus pelleted from infected cell
948 supernatant. The blots shown are representative. (d) Released viral titers were
949 quantified by FFU/ml assay from cells transfected with viral RNA transcribed from
950 cDNA for JFH-$1_{WT,}$ JFH-1_{W420A} and JFH-1_{W420V}. Panels a, b and d show average
951 values from duplicate independent experiments, error bars show SEM.
952
953 **Figure 2. Analysis of W420 mutants in the pseudoparticle system.**
954 Pseudoparticles were harvested from HEK cells transfected with wild type (WT), 420
955 mutant E1E2 or no envelope (NE). (a) HCVpp infectivity in Huh7 cells is expressed
956 as a percentage relative to wild type. The result shown is the average of 3 independent
957 experiments, error bars show SEM. (b) Representative western blot of pelleted wild
958 type and mutant HCVpp probed with anti-HCV E2 and anti-MLV Gag.
959
960 **Figure 3. Binding of E2 antibodies.** Reactivity of anti-E2 linear (a, b and c) and
961 conformational (d) antibodies with lysate from cells expressing wild type and mutant
962 E1E2 in GNA-ELISA. Bound antibodies were detected using secondary anti-species
963 antibodies conjugated to HRP. Background levels were removed by subtracting

964 binding of a lysate lacking E1E2. Each dataset shows the average of 3 independent
965 experiments, error bars show SEM.
966
967 **Figure 4. Neutralization by E2 antibodies.** JFH-$1_{WT,}$ JFH-1_{W420F} and JFH-1_{W420Y}
968 viruses were neutralized by mAb AP33 and mAb 3/11 that bind to $E2_{412-423}$ (a and b)
969 and by HmAb CBH-5 that binds immunodomain B (c). Each dataset shows the
970 average of 2 independent experiments, error bars show SEM.
971
972 **Figure 5. Virus-CD81 receptor interactions.** (a) Reactivity of sCD81-LEL in a
973 modified GNA-ELISA with the same panel of WT and mutant E1E2-containing
974 lysates as used in Fig. 3. Neutralization of JFH-$1_{WT,}$ JFH-1_{W420F} and JFH-1_{W420Y}
975 viruses by (b) anti-CD81 and (c) sCD81-LEL. Each dataset shows the average of 2
976 (b,c,d) or 3 (a) independent experiments, error bars show SEM.
977
978 **Figure 6. Virus-SR-BI receptor interactions.** Cell surface expression of the fusion
979 protein SR-BI.GFP was measured by detection of eGFP by flow cytometry. (a) The
980 filled grey peak represents CHO-SR-BI cells; the black line represents CHO-SR-
981 BI.GFP cells. Expression of human SR-BI was measured by comparing the binding of
982 by anti-SR-BI Mab151-NP1 (black line) and an IgG1 isotype control (filled grey
983 peak) to (b) CHO-K1, (c) CHO-hSR-BI and (d) CHO-hSR-BI.GFP cells. (e)
984 Neutralization of JFH-$1_{WT,}$ JFH-1_{W420F} and JFH-1_{W420Y} viruses by anti-SR-BI
985 Mab151-NP1. A dose-response curve of BLT-4 on (f) infectivity of JFH-$1_{WT,}$ JFH-
986 1_{W420F} and JFH-1_{W420Y} viruses and (g) cell viability. Each dataset shows the average of
987 2 (e) or 3 (f, g) independent experiments, error bars show SEM.
988

Figure 7: Virus-EGFR interactions. Dose-response curves for infectivity of JFH-$1_{WT,}$ JFH-1_{W420F} and JFH-1_{W420Y} viruses in the presence of (a) erlotinib, (c) anti-EGFR and (d, e) sunitinib. For panel (e) wild type and 420 mutant viruses were analyzed by student t-test, asterisks show statistically significant differences (* = $P<0.05$, ** = $P<0.05$). The dose-response analysis of cell viability is shown for (b) erlotinib and (f) sunitinib. Each dataset shows the average of 2 (c) or 3 (a,b,d,e,f) independent experiments, error bars show SEM.

Figure 8: Antibody-peptide interfaces. Detailed view of the interface between the common part of a synthetic E2 peptide (aa 413-423) with Fabs AP33 (left) and 3/11 (right), respectively. The Fab is colored according to a normalized hydrophobicity scale from white (hydrophobic) to orange (hydrophilic). The hydrogen bonds to carbonyl groups of residues NL91 (AP33) and TL96/TL97 (3/11) are shown as dashed black lines, these carbonyl groups are shown as sticks and colored in red.

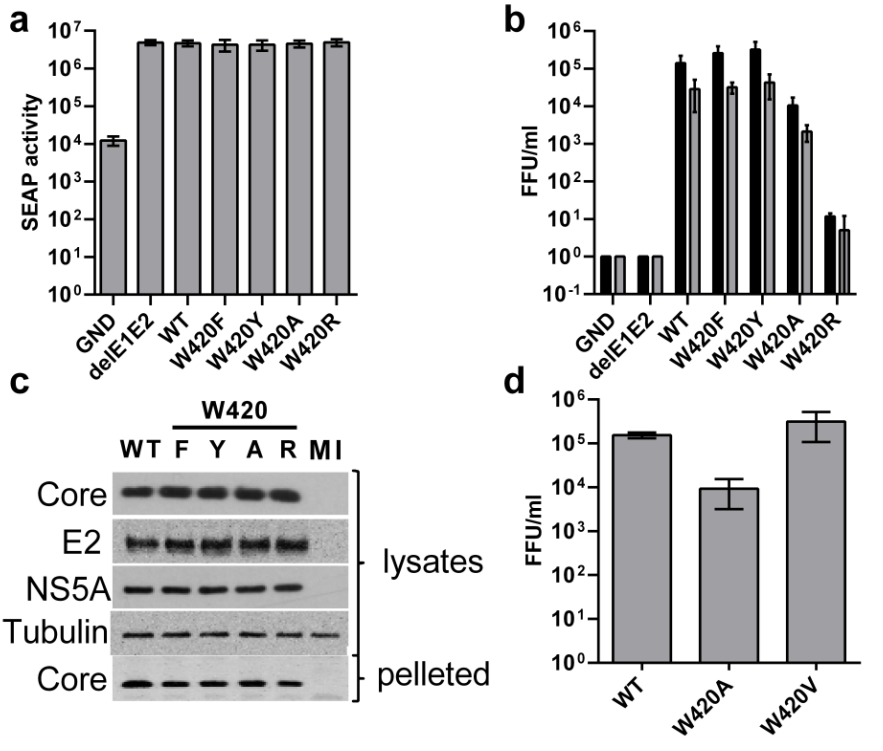

Figure 1. Analysis of W420 mutant viruses. Huh7 cells were transfected with viral RNA transcribed from cDNA encoding JFH-1_{WT}, JFH-1_{GND}, JFH-1_{DE1E2} and a panel of JFH-1_{W420} mutants and analyzed after 72h. (a) Intracellular viral replication was quantified by SEAP activity (RLU). (b) Viral titers were quantified by FFU/ml assay; black bars show extracellular virus harvested from the medium, grey bars show intracellular virus harvested from lysed cells. (c) Western blot analysis to detect (i) viral proteins Core, E2, NS5A and tubulin loading control in mock-infected (MI) and infected cell lysates and (ii) Core protein in released virus pelleted from infected cell supernatant. The blots shown are representative. (d) Released viral titers were quantified by FFU/ml assay from cells transfected with viral RNA transcribed from cDNA for JFH-$1_{WT,}$ JFH-1_{W420A} and JFH-1_{W420V}. Panels a, b and d show average values from duplicate independent experiments, error bars show SEM.

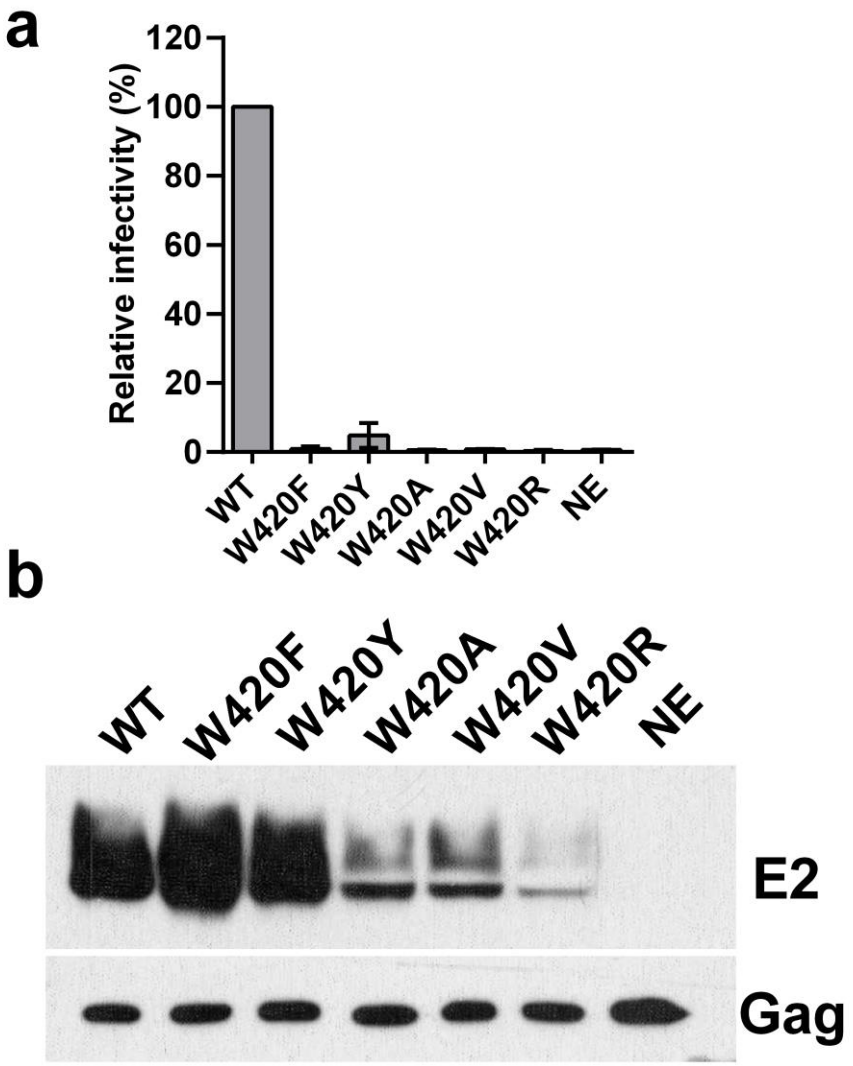

Figure 2. Analysis of W420 mutants in the pseudoparticle system. Pseudoparticles were harvested from HEK cells transfected with wild type (WT), 420 mutant E1E2 or no envelope (NE). (a) HCVpp infectivity in Huh7 cells is expressed as a percentage relative to wild type. The result shown is the average of 3 independent experiments, error bars show SEM. (b) Representative western blot of pelleted wild type and mutant HCVpp probed with anti-HCV E2 and anti-MLV Gag.

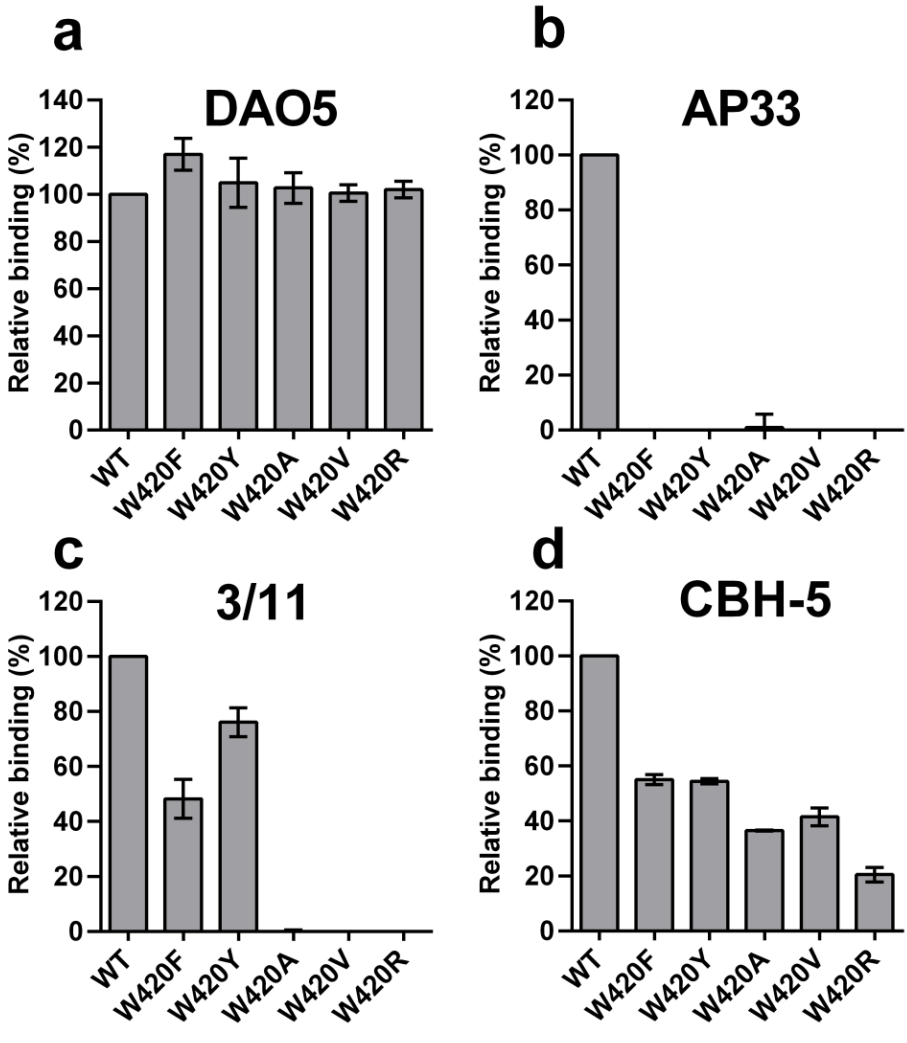

Figure 3. Binding of E2 antibodies. Reactivity of anti-E2 linear (a, b and c) and conformational (d) antibodies with lysate from cells expressing wild type and mutant E1E2 in GNA-ELISA. Bound antibodies were detected using secondary anti-species antibodies conjugated to HRP. Background levels were removed by subtracting binding of a lysate lacking E1E2. Each dataset shows the average of 3 independent experiments, error bars show SEM.

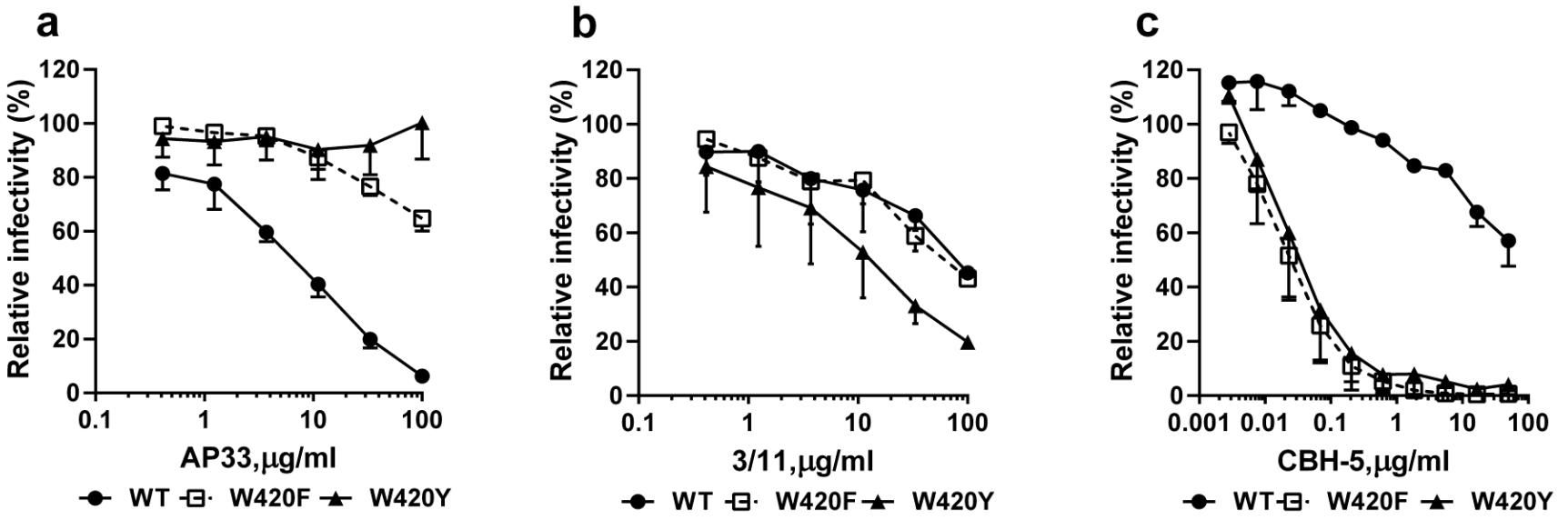

Figure 4. Neutralization by E2 antibodies. JFH-$1_{WT,}$ JFH-1_{W420F} and JFH-1_{W420Y} viruses were neutralized by mAb AP33 and mAb 3/11 that bind to $E2_{412-423}$ (a and b) and by HmAb CBH-5 that binds immunodomain B (c). Each dataset shows the average of 2 independent experiments, error bars show SEM.

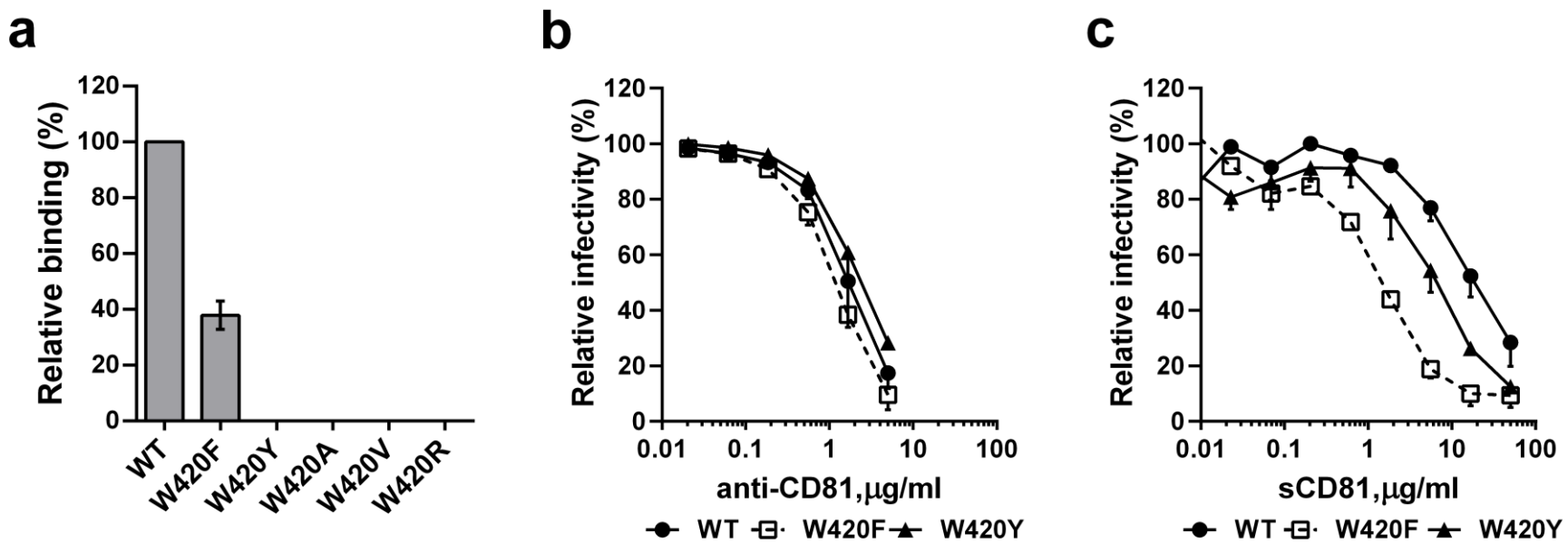

Figure 5. Virus-CD81 receptor interactions. (a) Reactivity of sCD81-LEL in a modified GNA-ELISA with the same panel of WT and mutant E1E2-containing lysates as used in Fig. 3. Neutralization of JFH-$1_{WT,}$ JFH-1_{W420F} and JFH-1_{W420Y} viruses by (b) anti-CD81 and (c) sCD81-LEL. Each dataset shows the average of 2 (b,c,d) or 3 (a) independent experiments, error bars show SEM.

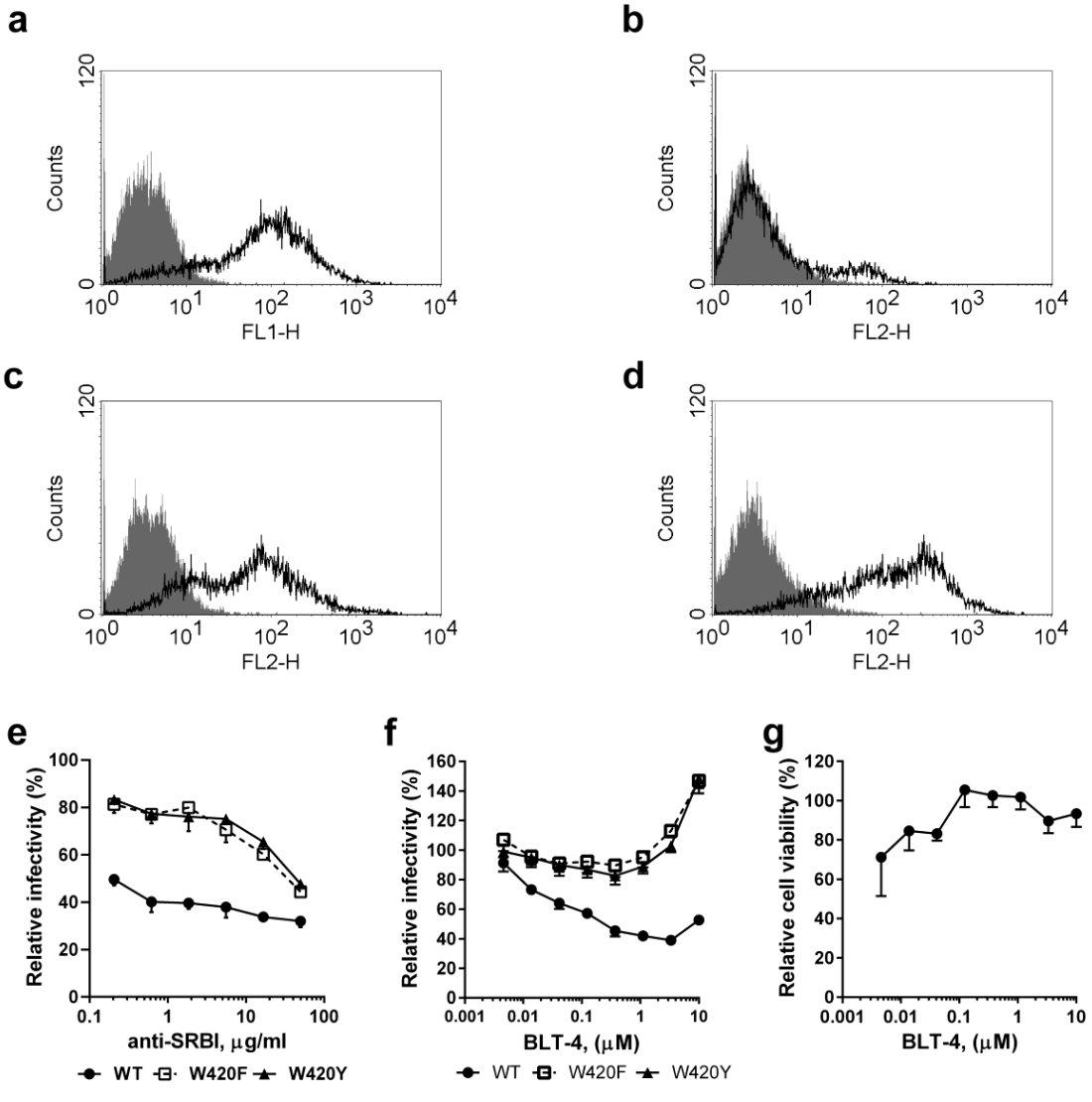

Figure 6. Virus-SR-BI receptor interactions. Cell surface expression of the fusion protein SR-BI.GFP was measured by detection of eGFP by flow cytometry. (a) The filled grey peak represents CHO-SR-BI cells; the black line represents CHO-SR-BI.GFP cells. Expression of human SR-BI was measured by comparing the binding of by anti-SR-BI Mab151-NP1 (black line) and an IgG1 isotype control (filled grey peak) to (b) CHO-K1, (c) CHO-hSR-BI and (d) CHO-hSR-BI.GFP cells. (e) Neutralization of JFH-$1_{WT,}$ JFH-1_{W420F} and JFH-1_{W420Y} viruses by anti-SR-BI Mab151-NP1. A dose-response curve of BLT-4 on (f) infectivity of JFH-$1_{WT,}$ JFH-1_{W420F} and JFH-1_{W420Y} viruses and (g) cell viability. Each dataset shows the average of 2 (e) or 3 (f, g) independent experiments, error bars show SEM.

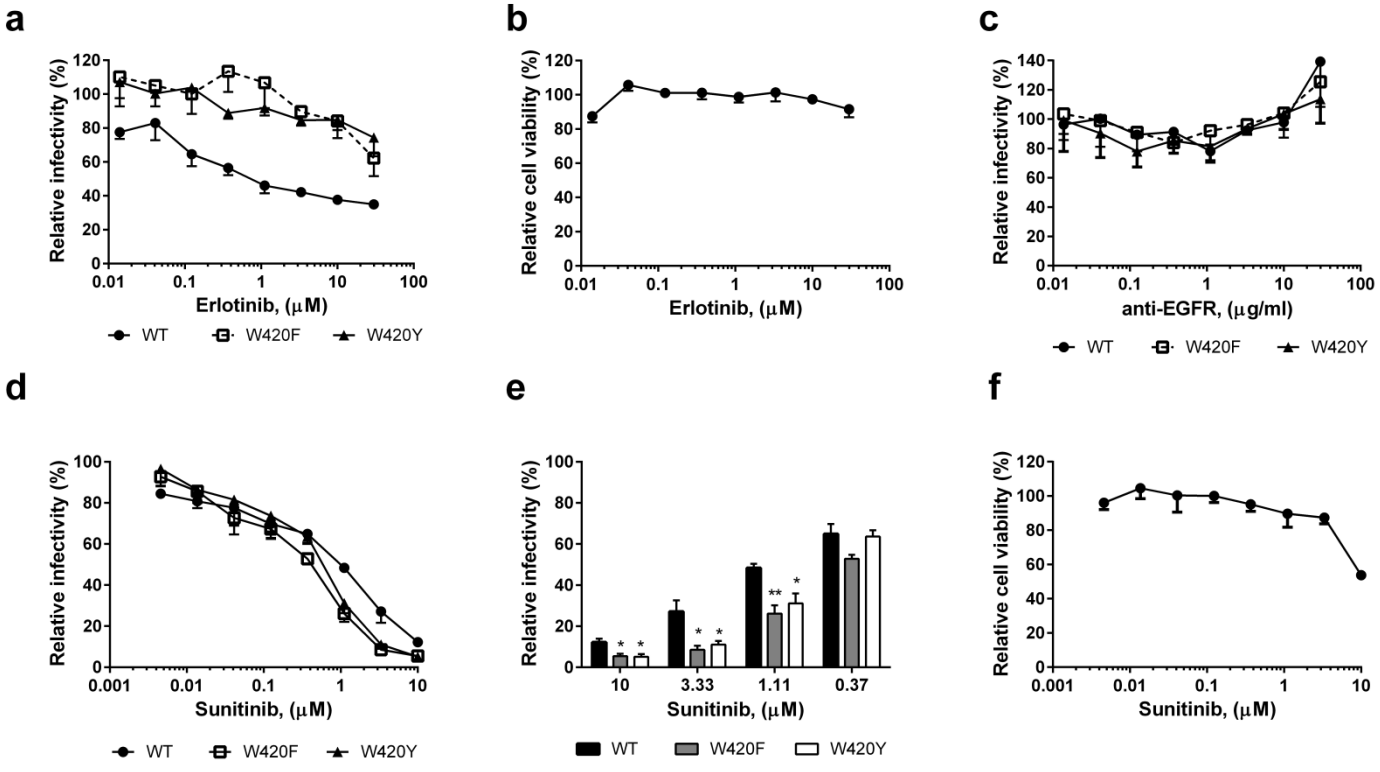

Figure 7: Virus-EGFR interactions. Dose-response curves for infectivity of JFH-$1_{WT,}$ JFH-1_{W420F} and JFH-1_{W420Y} viruses in the presence of (a) erlotinib, (c) anti-EGFR and (d, e) sunitinib. For panel (e) wild type and 420 mutant viruses were analyzed by student t-test, asterisks show statistically significant differences (* = P<0.05, ** = P<0.05). The dose-response analysis of cell viability is shown for (b) erlotinib and (f) sunitinib. Each dataset shows the average of 2 (c) or 3 (a,b,d,e,f) independent experiments, error bars show SEM.

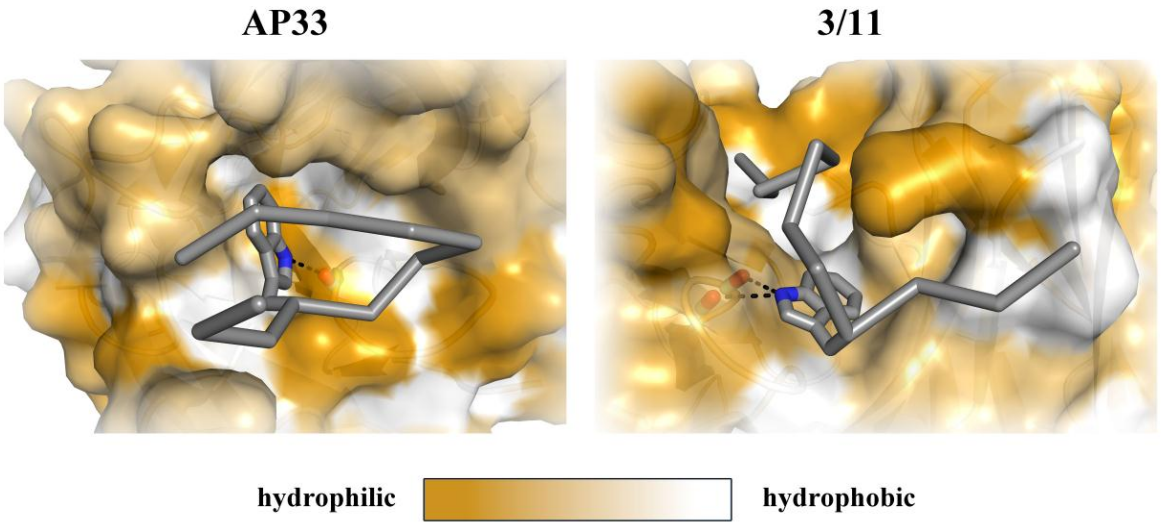

Figure 8. Antibody-peptide interfaces. Detailed view of the interface between the common part of a synthetic E2 peptide (aa 413-423) with Fabs AP33 (left) and 3/11 (right), respectively. The Fab is colored according to a normalized hydrophobicity scale from white (hydrophobic) to orange (hydrophilic). The hydrogen bonds to carbonyl groups of residues NL91 (AP33) and TL96/TL97 (3/11) are shown as dashed black lines, these carbonyl groups are shown as sticks and colored in red.